Tumor control in ion beam radiotherapy with different ions in the presence of hypoxia: an oxygen enhancement ratio model based on the microdosimetric kinetic model

Tumour control in ion beam radiotherapy with different ions in presence of hypoxia: an oxygen enhancement ratio model based on the microdosimetric kinetic model

L Strigari[1], F Torriani[2], L Manganaro[3], T Inaniwa[4], F Dalmasso[3,5], R Cirio[3,5], A Attili[5]‡

[1] Laboratory of Medical Physics and Expert Systems, National Cancer Institute Regina Elena, Roma, Italy

[2] Politecnico di Torino, Torino, Italy

[3] Physics Department, Università degli Studi di Torino, Torino, Italy

[4] National Institute for Quantum and Radiological Science and Technology, National Institute of Radiological Sciences, Department of Accelerator and Medical Physics, 4-9-1 Anagawa, Inage-ku, Chiba, 263-8555, Japan

[5] Istituto Nazionale di Fisica Nucleare (INFN) Sez. di Torino, Torino, Italy

E-mail: attili@to.infn.it

Abstract. Few attempts to include the oxygen enhancement ratio (OER) in treatment planning for ion beam therapy have been made and systematic studies to evaluate the impact of hypoxia in treatments with beam of different ion species are highly needed. The radiobiological models used to quantify the OER in such studies are mainly based on the dose-averaged LET estimates and do not explicitly distinguish between ion species and fractionation schemes. In this study a new OER modelling, based on the microdosimetric kinetic model, taking into account the specificity of the different ions, LET spectra, tissues and fractionation schemes, has been developed. The model has been benchmarked with published in-vitro data, HSG, V79 and CHO cells in aerobic and hypoxic conditions, for different ions irradiation. The model has been included in the simulation of treatments for a clinical case (brain tumor) using proton, lithium, helium, carbon and oxygen ion beams. A study of the tumour control probability (TCP) as a function of oxygen partial pressure, dose per fraction and primary ion type has been performed. The modeled OER depends on both LET and ion type, showing also a decrease for increasing dose per fraction with a slope that depends on the LET and ion type, in good agreement with the experimental data. In the investigated clinical case, a significant increase in TCP by increasing ion charge has been found. Higher OER variations as a function of dose per fraction have been also found for low-LET ions (up to 15% varying from 2 to 8 Gy(RBE) for protons). The model could be exploited for the identification of the treatment condition optimality in presence of hypoxia, including fractionation and primary particles selection.

PACS numbers: 87.53, 87.55

‡ Author to whom any correspondence should be addressed.

Keywords: OER, Ion Beam Therapy, Treatment Planning, RBE

1. Introduction

It has become well established that the response of cells to ionizing radiation is strongly dependent upon oxygenation condition. In particular, a significantly lower cell death rate after exposure to ionizing radiation is observed in presence of a reduced concentration of oxygen in cells, *i.e.* in hypoxic conditions. As clinically observed, solid tumours could contain oxygen-deficient regions, thus increasing their radioresistance and potentially leading to treatment failure, *i.e.* lacking of tumoural control (Thomlinson & Gray 1955, Hockel et al. 1993). This condition is mainly related to two different mechanisms indicated as chronic or acute hypoxia. The chronic hypoxia is due to the limited diffusion distance of oxygen while the acute hypoxia is caused by a temporary closure of a tumour blood vessel and is a transient condition (Held 2006).

The radioresistance induced by hypoxia can be quantified by the oxygen enhancement ratio, OER, a parameter defined as the ratio between the radiation dose in hypoxic conditions, D_h, and the radiation dose in aerobic conditions, D_a, that produces the same biological effect, S:

$$\mathrm{OER} = \left.\frac{D_h(p_h)}{D_a}\right|_S \tag{1}$$

where p_h is the oxygen partial pressure of the hypoxic phase. In this study we focused on the OER variation according to the oxygen concentration, studying the required isoeffective dose in the hypoxic phase with respect to the fixed reference dose required in the aerobic phase.

It has been observed that the OER depends on many other factors such as the tissue type, the linear energy transfer (LET) of the radiation and the cell surviving fraction (or alternatively the applied local dose). In particular, the OER decreases progressively with the increase of LET and, for high-LET radiation, the survival of tumour clonogenic cells is less affected by oxygen concentration (Raju et al. 1978, Ando et al. 1999, Nakano et al. 2006). Ion beam therapy, due to the high LET characteristics of this radiation, is foreseen as a promising technique to overcome hypoxic radioresistance.

To design better interventions in presence of hypoxia, a proper modelling of the mechanism of radioresistance is fundamental. This high-LET phenomenon has not yet been fully understood and, up to now, a consistent (uniform/general) theory, which might explain the OER on a biological and physical basis, has not been accepted yet, though several models have been proposed to explain this effect (Ward 1994, Michael & Prise 1996, Stewart et al. 2011, Bopp et al. 2016). Some of them suppose a radiolytic formation of an oxygenated microenvironment around the high-LET tracks as the factor responsible for the OER reduction with the increase of LET (Meesungnoen & Jay-Gerin 2009).

Other relevant approaches to OER modelling, more oriented to treatment planning evaluations, have been proposed by (Wenzl & Wilkens 2011*a*), (Scifoni et al. 2013) and (Antonovic et al. 2013). These models are mainly phenomenological and the following limits can be identified. The main OER predictors are based on the dose-

averaged LET (LETd), used as a surrogate of the full spectra. The LETd approximates the contribution of secondary fragments and the variable complex spectra that can be usually found in the irradiation field of a clinical treatment. Although an OER dependence on the ion type has been experimentally observed in the Z range from He to Ne (Furusawa et al. 2000), this effect is not explicitly accounted for in the proposed models. This effect could be relevant for light particles (proton and helium ions), while Furusawa *et al.* (2000) observed a small OER dependence for a Z range from C to Ne and other authors (Tinganelli et al. 2013) found a negligible dependence from C to O.

Notably, the OER dependence on ion type has been accounted in a recent proposed model, concomitant with the present work, in which a reformulation of the microdosimentric kinetic model (MKM) (Hawkins 1998, Hawkins 2003, Inaniwa et al. 2010) has been developed to include the effects of oxygen (Bopp et al. 2016). Briefly, this formulation rely heavily on the knowledge of the OER function for damages caused by low-LET particles such as photons (*photon OER*). The damage reduction due to hypoxia in the case of ions irradiation is obtained from this function to modulate the initial lethal and potentially lethal lesions in the cell, assumed to vary as the inverse of the *photon OER*. Other parameters of the MKM, the effective domain and nucleus sizes, are modulated proportionally to the *photon OER*. At the present, this model has been applied only to a limited data set. In particular, no predictions and experimental comparisons of the OER as a function of oxygen partial pressure have been performed and the expected OER dependence on LET is still controversial, predicting an increasing OER for high LET (LET $\geq$ 400 keV/μm). In addition, with the exceptions of a theoretical study in (Wenzl & Wilkens 2011*b*), these models are also limited to predict the OER at a fixed surviving fraction (10%) that could be not representative of the cell survival at the commonly clinically used dose per fraction.

In order to better exploit the characteristics of ions in treatments, a more complete OER model is required. The observed dependence on ion type suggests to include the track structure effects in a more mechanistic modelling of the oxygen effect. This aspect can be of particular importance in order to optimize ion-based treatment planning according to the grade of hypoxia expected in the tumour.

In this study, an alternative model, based on the MKM and using a complementary approach to the one reported in (Bopp et al. 2016), has been developed to evaluate the OER in the case of irradiation with different ions. The model has been benchmarked with *in vitro* experimental data (Furusawa et al. 2000, Tinganelli et al. 2015). In a second part of the study, the model has been included in treatment simulation of a brain tumour, to evaluate the potential benefits of different ion types (H, He, Li, C and O) in presence of hypoxia in terms of tumour control probability (TCP).

2. Materials and methods

2.1. Oxygen enhancement ratio (OER) modelling

2.1.1. Linear quadratic model and OER dependence on survival According to the linear quadratic (LQ) model (Kellerer & Rossi 1978) the fraction S of cells that survive an applied dose D may be written as:

$$-\ln S = \alpha D + \beta D^2 \tag{2}$$

where α and β are two general radiosensitivity parameters. Following the definition in equation 2, by equating the surviving fractions for aerobic and hypoxic cells $S_a(D_a) = S_h(D_h) = S$, it is possible to express the OER as a function of the cell survival

$$\mathrm{OER} = \frac{\sqrt{\alpha_h^2 - 4\beta_h \ln S} - \alpha_h}{\sqrt{\alpha_a^2 - 4\beta_a \ln S} - \alpha_a} \times \frac{\beta_a}{\beta_h} \tag{3}$$

where (α_a, β_a) and (α_h, β_h) are the specific LQ parameters for aerobic and hypoxic conditions respectively. Following equation 3, the OER dependence from tissue type, LET, ion type and oxygen partial pressure p can be included through a proper modelling of these radiosensitivity parameters.

2.1.2. α and β dependence on oxygen partial pressure To express the OER dependence on the oxygen partial pressure, a parametrization of α and β is introduced, following an idea originally reported in (Wenzl & Wilkens 2011*a*). Following an equivalent formulation by (Alper & Howard-Flanders 1956) of the relative radiosensitivity as a function of the oxygen partial pressure p, the OER can be written in the form

$$\mathrm{OER}(p) = \frac{p + K}{p + K \times \mathrm{OER}_{\max}^{-1}} \tag{4}$$

where $\mathrm{OER}_{\max}$ is the maximum OER value in the limit $p \to 0$ and K is the oxygen partial pressure at which the mean of the relative sensitization and 1 is achived. $K = 3$ mmHg has been experimentally determined from photon data for different cell lines (Wouters & Brown 1997, Held 2006, Jones et al. 2007) and used in this analysis. By using equations 1 and 2, the effect of oxygen partial pressure on hypoxic cell survival can be incorporated into the LQ formalism by modifying α and β accordingly to

$$-\ln S = \alpha_{\max} D/\mathrm{OER}(p) + \beta_{\max} D^2/\mathrm{OER}^2(p) \tag{5}$$

where $\alpha_{\max}$ and $\beta_{\max}$ are the parameters describing the extrapolated response for high oxygen partial pressure ($p \to \infty$). These parameters are similar but numerically different from α_a and β_a of the reference (normoxic) phase, since the latter correspond to a finite value of partial pressure. To account for the OER dose dependence, a generalization of equation 5 is introduced by using separate functions for α and β (Wouters & Brown 1997)

$$-\ln S = \alpha_{\max} D/\mathrm{OER}_\alpha(p) + \beta_{\max} D^2/\mathrm{OER}_\beta^2(p) \tag{6}$$

Using equations 4 and 6 is possible to extrapolate the LQ parameters as functions of an arbitrary oxygen partial pressure p by

$$\alpha(p) = \frac{p\alpha_{\max} + K\alpha_{\min}}{p + K} \tag{7}$$

and

$$\sqrt{\beta(p)} = \frac{p\sqrt{\beta_{\max}} + K\sqrt{\beta_{\min}}}{p + K} \tag{8}$$

where $\alpha_{\min} = \alpha_{\max}/\mathrm{OER}_{\max}^{(\alpha)}$ and $\beta_{\min} = \beta_{\max}/\mathrm{OER}_{\max}^{(\beta)}$ correspond to the limit $p \to 0$, see also (Wenzl & Wilkens 2011*a*). From equations 7 and 8 is possible to identify $\alpha_a = \alpha(p_a)$, $\beta_a = \beta(p_a)$, $\alpha_h = \alpha(p_h)$ and $\beta_h = \beta(p_h)$ in equation 3, where p_h and p_a are the oxygen partial pressures in the hypoxic and aerobic phase, respectively.

Following the original idea by (Wenzl & Wilkens 2011*a*), the dependence of OER on the LET is introduced at the level of the LQ parameters $\alpha_{\max}$, $\alpha_{\min}$, $\beta_{\max}$ and $\beta_{\min}$ with a proper modelling choice. While in the cited paper a simple linear model was adopted, in the present study an approach based on the MKM was followed. The details are given in the next sections.

2.1.3. Microdosimetric kinetic model (MKM) formulation To evaluate the parameters $(\alpha_{\max}, \beta_{\max})$ and $(\alpha_{\min}, \beta_{\min})$ in equations 7 and 8 in case of irradiation with ion beams, a formulation of the MKM has been considered, in which an amorphous track model has been taken into account to evaluate the stochastic energy deposition at the micrometric scale. Details of the model are reported elsewhere (Kase et al. 2008), and only the relevant features of the model are briefly highlighted here. The application of the MKM in the context of the OER modelling has already been proposed elsewhere (Bopp et al. 2016). The present modelling represents a complementary and substantially different approach to the one presented in the cited work.

The MKM assumes a Poissonian process for the cell survival

$$S = \exp(-\langle L_n \rangle) \tag{9}$$

where $\langle L_n \rangle$ represents the cellular population averaged number of lethal lesions in the nucleus, which is the sum of the number of lesions in all domains (sub-functional units of the cell nucleus). For each domain the number of lesions is given by a LQ function of the specific energy, $Az + Bz^2$, for any radiation type. The LQ parameters, A and B, are dependent on the cell type and z is the sum of the single-track specific energies, z_1, for each domain. When the Poisson distribution is assumed for the lethal event of the domain, the average $\langle L_n \rangle$ is given by

$$\langle L_n \rangle = (\alpha^0 + \beta^0 \bar{z}_{1D})D + \beta^0 D^2 = \alpha_p D + \beta^0 D^2 \tag{10}$$

where α^0 and β^0 are parameters related to A and B, that do not depend on the radiation type, but only on the cell type. D is the macroscopic adsorbed dose and $\bar{z}_{1D}$ is the dose averaged z_1 over the domains.

In case of high LET particles, a correction factor due to the non-Poisson lethal event distribution is introduced for the linear term (Hawkins 2003, Kase et al. 2008)

$$\alpha = (1 - \exp(-\alpha_p \bar{z}_{1Dn})) \, \frac{\alpha_p}{\bar{z}_{1Dn}} \tag{11}$$

where $\bar{z}_{1Dn}$ is the single-track dose averaged specific energy deposited in the nucleus.

The correct determination of the ratio $\sqrt{\beta_a/\beta_h}$ through the quadratic components in equation 8 could be relevant in the study of the OER for high doses per fraction. In the original formulation of the MKM the parameter β is assumed to be LET independent and no high-LET corrections are applied, *i.e.* $\beta = \beta^0$. This could be a crude approximation for very high LET irradiation where a vanishing β has been observed experimentally (Furusawa et al. 2000).

In the present study we introduced a LET dependence in the parameter β adopting the same conceptual approach used in the case of Local Effect Model (LEM) (Krämer & Scholz 2006). Using the present mathematical notation, this approach assumes the relation

$$\beta = (\alpha/\alpha_p)^2 \beta_p \tag{12}$$

where α_p and $\beta_p = \beta^0$ are the Poisson LQ parameters defined in equation 10, while α and β are the non-Poisson corrected parameters. Equation 12 expresses the *ansatz* that the same scaling between α and α_p should apply between β and β^0, but squared since the β-terms are associated with the dose squared. This is obviously an approximation, however it represents an improvement with respect the constant β used in the original formulation of the MKM. In particular, using equation 12 a vanishing β for high LET can be reproduced.

2.1.4. α and β dependence on LET and ion type The LET and ion type dependence is introduced in equations 10, 11 and 12 via the quantities $\bar{z}_{1D} = \bar{z}_{1D}(Z, \mathrm{LET})$ and $\bar{z}_{1Dn} = \bar{z}_{1Dn}(Z, \mathrm{LET})$, where Z is the atomic number. These dependences rely on the specific adopted track model. Following the work of (Kase et al. 2008) an amorphous track model is obtained by the combination of the Kiefer model for the penumbra region (Kiefer & Straaten 1986) and the Chatterjee model for the core radius (Chatterjee & Schaefer 1976). In this model the core radius R_c (μm), the penumbra radius R_p (μm) and the dose D_{KC} as function of track radius r (μm) are evaluated as follows

$$R_c = 0.0116 \times \beta_{\mathrm{ion}} \tag{13}$$

$$R_p = 0.0616 \times (E_s)^{1.7} \tag{14}$$

$$D_{\mathrm{KC}}(r \le R_c) = \frac{1}{R_c^2} \left(\frac{\mathrm{LET}_\infty}{r\rho} - 2\pi K_p \ln(R_p/R_c) \right) \tag{15}$$

$$D_{\mathrm{KC}}(r > R_c) = 1.25 \times 10^{-4} (z^*/\beta_{\mathrm{ion}})^2 r^{-2} \tag{16}$$

where E_s is the specific energy in MeV/u, z^* is the effective charge given by the Barkas expression, β_{ion} is the velocity relative to the speed of light, LET_∞ is the unrestricted LET and ρ is the density of water. In order to evaluate the averages of the imparted

energies, the domain and nucleus are assumed to have a cylindrical symmetry with the direction of the incident ion parallel to the cylinder axis

$$\bar{z}_{1D} = \int_0^{b_{\max}} D(b)^2 b \, \mathrm{d}b \Big/ \int_0^{b_{\max}} D(b) b \, \mathrm{d}b \tag{17}$$

$$\bar{z}_{1Dn} = \int_0^{b_{\max}^{(n)}} D_n(b)^2 b \, \mathrm{d}b \Big/ \int_0^{b_{\max}^{(n)}} D_n(b) b \, \mathrm{d}b \tag{18}$$

where $D(b)$ and $D_n(b)$ are the doses for a single track with impact parameter b evaluated via the integration of D_{KC} in the domain and in the nucleus respectively, and $b_{\max}$ and $b_{\max}^{(n)}$ are the maximum impact parameters to have a non negligible energy deposition in the domain and in the nucleus respectively. These parameters, or equivalently the radius of the domain R_d and of the nucleus R_n, represents two additional parameters of the model and are associated to a specific cell type.

2.1.5. MKM formulation for the OER The general expressions for the parameters $\alpha_{\max}$, $\alpha_{\min}$, $\beta_{\max}$ and $\beta_{\min}$ in equations 7 and 8 as functions of LET, ion type and tissue type, are obtained by using the MKM equations described in 10, 11, 12, 17 and 18 by means of a proper choice of the corresponding set of parameters $(\alpha^0_{\max}, \beta^0_{\max}, \alpha^0_{\min}, \beta^0_{\min}, R_n, R_d)$

$$\alpha_{\max} = \alpha(\mathrm{LET}, Z; \alpha^0_{\max}, \beta^0_{\max}, R_n, R_d) \tag{19}$$

$$\alpha_{\min} = \alpha(\mathrm{LET}, Z; \alpha^0_{\min}, \beta^0_{\min}, R_n, R_d) \tag{20}$$

$$\beta_{\max} = \beta(\mathrm{LET}, Z; \alpha^0_{\max}, \beta^0_{\max}, R_n, R_d) \tag{21}$$

$$\beta_{\min} = \beta(\mathrm{LET}, Z; \alpha^0_{\min}, \beta^0_{\min}, R_n, R_d) \tag{22}$$

where R_n and R_d, representing the cell geometrical attributes, are considered the same for all the LQ parameters.

We remark that, in the present modelling, there is a complete decoupling between the physical track description and the biological parameters ($\alpha^0_{\max}$, $\alpha^0_{\min}$, $\beta^0_{\max}$ and $\beta^0_{\max}$), which describe the biological response of the cell at the micrometric level. In this decoupling, the track model only takes into consideration the physical aspects of the irradiation and do not consider the associated radiochemical process. These last processes, which play a major role in the modulation induced by the presence of oxygen, are accounted effectively through phenomenological estimates of the biological parameters of the model. In particular, the ratio $\alpha^0_{\max}/\alpha^0_{\min}$ represents the maximum theoretical OER ($\mathrm{OER}_{\max}$ in equation 4) in the limit $\mathrm{LET} \to 0$ and $D \to 0$, while the ratio $\sqrt{\beta^0_{\max}/\beta^0_{\min}}$ represents the $\mathrm{OER}_{\max}$ in the limit $\mathrm{LET} \to 0$ and $D \to \infty$. We further remark that this kind decoupling is a characteristic inherent of the MKM and it is also present in the MKM-based approach described in (Boop et al. 2016), although the way in which the biological parameters are modulated is different.

2.1.6. Model validation To establish an experimental reference for the proposed model, the calculated OER values have been benchmarked with the published *in vitro* dataset (Furusawa et al. 2000), in which several cell survival measurements in both aerobic and hypoxic condition for He, C and Ne ions are reported as a function of the LET. The model was fitted to reproduce the OER for two exemplary tissues, V79 and human salivary gland (HSG) cells irradiated with different ions. The modelled OER dependence on the oxygen partial pressure has been benchmarked using the survival dataset of chinese hamster ovary (CHO) cells exposed to different ions in oxygen concentration ranging from normoxia (21%) to anoxia (0%) published in (Tinganelli et al. 2015).

2.2. Treatment simulations

2.2.1. Treatment planning implementation The treatment simulations have been carried out using a treatment planning system (TPS) for ion beam therapy with active scanning developed by INFN (Russo et al. 2016). This TPS incorporates a modelling approach, the beamlets superposition (BS) model, specifically conceived to allow the simulation of beams of different ion types and complex energy spectra, including the nuclear fragmentation that produces a progressive build-up of secondary ions along the penetration depth in the tissue. In the BS model each ion beam has been though as composed of sub-units, called beamlets, which are splitted into groups of ions. When the beam crosses a material, then the total irradiation effect is computed superimposing or averaging the separate beamlets effects. The beamlets may have either dimension comparable with the beam, or very small, in the limit coincident with the single particles. Track distributions were generated using Monte Carlo simulations in a water phantom irradiated with monoenergetic beams. These distributions, collected in look-up tables, are then recombined in the patient geometry using the BS approach and a water equivalent path length approximation. More details are described in (Russo et al. 2016).

To evaluate the OER, three dimensional distribution of a complete treatment irradiation, the average quantities $\bar{\alpha}_{\max}$, $\bar{\alpha}_{\min}$, $\bar{\beta}_{\max}$ and $\bar{\beta}_{\min}$ have to be evaluated for each voxel (indexed by v) of the target *i.e.* hypoxic volume. The beamlets superposition is carried out by applying the mixed-field formalism (Zaider & Rossi 1980) at the level of the single tracks (indexed by t)

$$\bar{\alpha}_{\max,v} = \frac{\sum_t \mathrm{LET}_t \alpha(\mathrm{LET}_t, Z_t; \alpha^0_{\max}, \beta^0_{\max}, R_n, R_d)}{\sum_t \mathrm{LET}_t} \tag{23}$$

$$\bar{\alpha}_{\min,v} = \frac{\sum_t \mathrm{LET}_t \alpha(\mathrm{LET}_t, Z_t; \alpha^0_{\min}, \beta^0_{\min}, R_n, R_d)}{\sum_t \mathrm{LET}_t} \tag{24}$$

$$\bar{\beta}_{\max,v} = \left(\frac{\sum_t \mathrm{LET}_t \sqrt{\beta(\mathrm{LET}_t, Z_t; \alpha^0_{\max}, \beta^0_{\max}, R_n, R_d)}}{\sum_t \mathrm{LET}_t} \right)^2 \tag{25}$$

$$\bar{\beta}_{\min,v} = \left(\frac{\sum_t \mathrm{LET}_t \sqrt{\beta(\mathrm{LET}_t, Z_t; \alpha^0_{\min}, \beta^0_{\min}, R_n, R_d)}}{\sum_t \mathrm{LET}_t} \right)^2 . \tag{26}$$

2.2.2. Spread out Bragg peak simulations (SOBP) in simplified geometries With the aim of evaluating OER distributions and its dependencies of the position and size of the hypoxic region, the model has been applied to a simplified case in which the irradiated volume consists of 170 mm wide cubic water phantom, with a completely hypoxic smaller cubic tumoural target volume (HTV), 40 mm wide, located in the phantom center.

The SOBP was optimized to deliver 2 Gy in the target region using an unilateral irradiation field. The oxygen partial pressure has been set to 0.01 mmHg for the hypoxic conditions, while a partial pressure of 160 mmHg has been considered for the reference aerobic conditions. Those partial pressures correspond to the experimental conditions for in-vitro measurements as reported in (Furusawa et al. 2000).

Two analyses have been conducted. In the first analysis, the size of the target has been varied setting the edge of the HTV to 20, 40, and 60 mm, in order to evaluate the OER sensitivity to the SOBP size in the phantom. In the second analysis, the position of the HTV region has been modified in order to evaluate the OER sensitivity to the SOBP depths in the phantom. The following HTV position shifts have been considered: -50, 0, and 50 mm with respect to the isocenter placed at the center of the cube.

2.2.3. Clinical treatment simulations To evaluate the OER and the impact of hypoxia in a clinical treatment, a brain tumour case has been studied. The irradiation has been performed using three fields coplanar to the coronal plane, with gantry angles of 90, 27 and 90 degrees and corresponding patient support angles of 270, 40 and 320 degrees, respectively (see figure 6).

The hypoxic region has been located in the center of the tumour area and modelled by shrinking the clinical target volume (CTV) using a 1 mm margin, while the planning target volume (PTV) was defined by increasing the size of the CTV considering a 5 mm margin. Different values of the oxygen partial pressure in the HTV have been considered to simulate different clinical hypoxia conditions, from low hypoxia, $p_h = 20$ mmHg, to high hypoxia, $p_h = 0.5$ mmHg (Nakano et al. 2006, McKeown 2014). For the aerobic condition, the clinic normoxic condition corresponding to oxygen partial pressure of $p_a = 30$ mmHg has been used.

The patient has been treated with different ion beams (H, He, Li, C, O) and different relative biological effectiveness RBE-weighted doses (RWD) per fraction in the planning target volume (PTV): 2, 4, 6 and 8 Gy(RBE_a)/fraction. With the notation "Gy(RBE_a)" we indicate that the RWD was optimized assuming a RBE relative to the photon reference irradiation for the normoxic conditions for which the OER = 1. The effect of hypoxia was evaluated through a generalization of the concept of the RBE and RWD by means of a further relative modulation of the biological effect described by the OER

$$\mathrm{RBE}_h(D, p_h) = \frac{\mathrm{RBE}_a(D)}{\mathrm{OER}(D, p_h)} \tag{27}$$

The normoxic RBE (RBE_a) has been evaluated using the same MKM implementation described in sections 2.1.1 and 2.1.2, specifically parametrized for a generic reference

normoxic tissue, characterized by the ratio of LQ parameters for the photon irradiation $\alpha_X/\beta_X = 3$ Gy. The parametrization used for the OER evaluations has been obtained via a fit of *in-vitro* data for the CHO cell line taken at different oxygen concentrations (see section 3.1.3). RWD in presence of hypoxia is evaluated as

$$\mathrm{RWD}(D, p_h) = D \times \mathrm{RBE}_h(D, p_h). \tag{28}$$

2.2.4. Tumour control probability (TCP) evaluation The model used to quantify the TCP is based on a Poisson process and unicellular hypothesis assumptions (Munro & Gilbert 1961). Within these assumptions, the TCP is formulated as a product of the probabilities

$$\mathrm{TCP} = \prod_{dv \in \mathrm{CTV}} P(D(v), p_h(v))^{\mathrm{d}v} \tag{29}$$

where the product is over the sub-volume dv included in the CTV. The voxel-based probabilities are functions of the generalized RWD found in each voxel (see equations 27 and 28) and are formulated through the LQ formalism

$$P(D, p_h) = \exp\left(-\exp(e\gamma - \alpha_X \mathrm{RWD}(D, p_h) - \beta_X \mathrm{RWD}(D, p_h)^2/n)\right) \tag{30}$$

where α_X and β_X are the LQ parameters associated to the tumour for the photon reference irradiation, γ is a parameter associated to the density of clonogenic cells in the tumour and n is the number of fractions of the treatment. In the present analysis the tumour is considered uniformly radioresistant through the definition of a unique LQ parametrization through the tumour volume, while the effect of variable hypoxia is implicitly included in the generalized RWD. The parameter values are: $\alpha_X = 0.075$ Gy^{-1}, $\beta_X = 0.025$ Gy^{-2} and $\gamma = 2$, corresponding to a threshold dose $D50 = 52.8$ Gy(RBE) (Bentzen & Tucker 1997).

3. Results

3.1. OER model benchmark on in-vitro data

3.1.1. LET and ion type dependence The calculated OER for HSG cells irradiated with different ions as a function of LET is reported in figure 1 and benchmarked with the published *in vitro* dataset (Furusawa et al. 2000). In the same figure, the OER calculated with the models proposed in (Wenzl & Wilkens 2011*a*, Scifoni et al. 2013) are reported for comparison. In figure 2 a similar analysis is performed with V79 cells. In this case, an additional comparison with the model proposed in (Antonovic et al. 2013) is also reported. The MKM-based model parameters corresponding to the two cell lines are reported in table 1. The obtained parametrizations are independent on the ion type and depends solely on the selected cell line.

The following fixed oxygen partial pressures have been used for the calculations: $p_h = 0.01$ mmHg for the cells in hypoxic conditions and $p_a = 160$ mmHg for the aerobic conditions, corresponding to values reported in the experimental study. Furthermore,

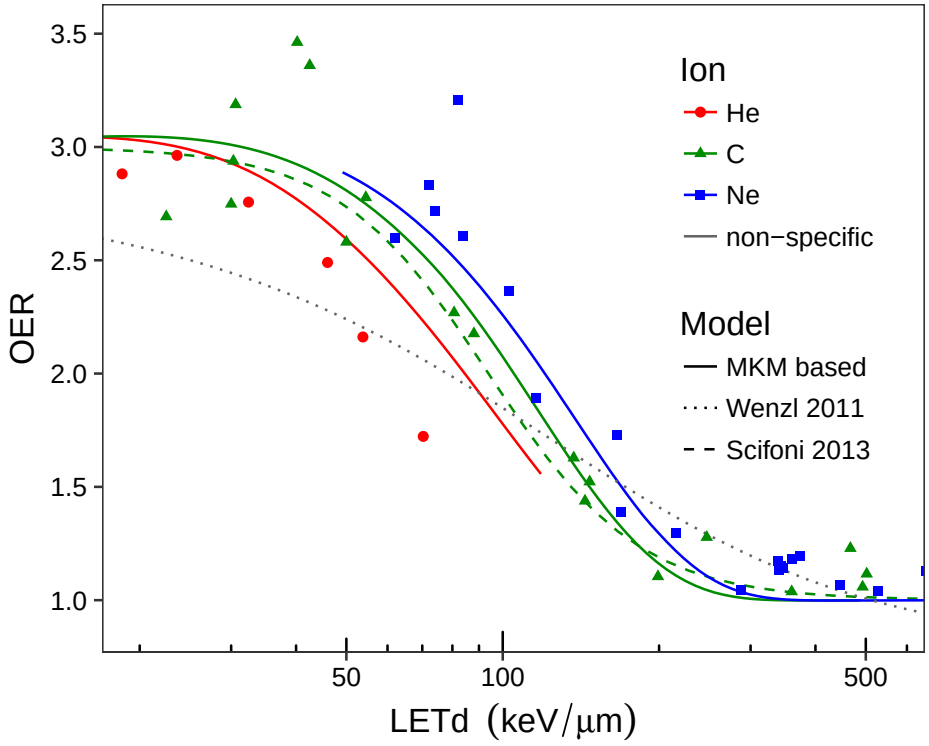

Figure 1. OER as a function of dose averaged LET for the irradiation of HSG cells with different ions. Points represent experimental data taken from (Furusawa et al. 2000). Continuous coloured lines represent the OER simultaneously evaluated by means of the MKM-based model for He, C and Ne. In the same plot the OER calculated with other models are reported for comparison (non-continuous lines). The model by (Scifoni et al. 2013) is associated with carbon ions only (green curve), while the model by (Wenzl & Wilkens 2011*a*) is not associated to a specific ion (grey curve.)

Table 1. MKM parameters for HSG, V79 and CHO cells.

Cell line	$\alpha^0_{\max}$ (Gy^{-1})	$\alpha^0_{\min}$ (Gy^{-1})	$\beta^0_{\max}$ (Gy^{-2})	$\beta^0_{\min}$ (Gy^{-2})	R_n (μm)	R_d (μm)
HSG	0.763	0.024	0.129	0.049	3.97	0.36
V79	0.799	0.011	0.117	0.051	4.56	0.31
CHO	0.525	0.066	0.044	0.020	3.91	0.22

the experimental OERs and the corresponding evaluations are obtained for a fixed survival level of 10%.

We also observed that some approximations commonly used in the MKM, specifically those used in the evaluation of the single-event averaged specific energies z_{1D} and z_{1Dn} (equation 17 and 18), have an impact on the OER predictions. In particular, we verified that by using the approximation introduced by (Hawkins 2003) and used in (Kase et al. 2008) for the single-event averaged specific energy at the nucleus level,

$$z_{1Dn} = \mathrm{LET}_\infty / \rho \sigma_N, \tag{31}$$

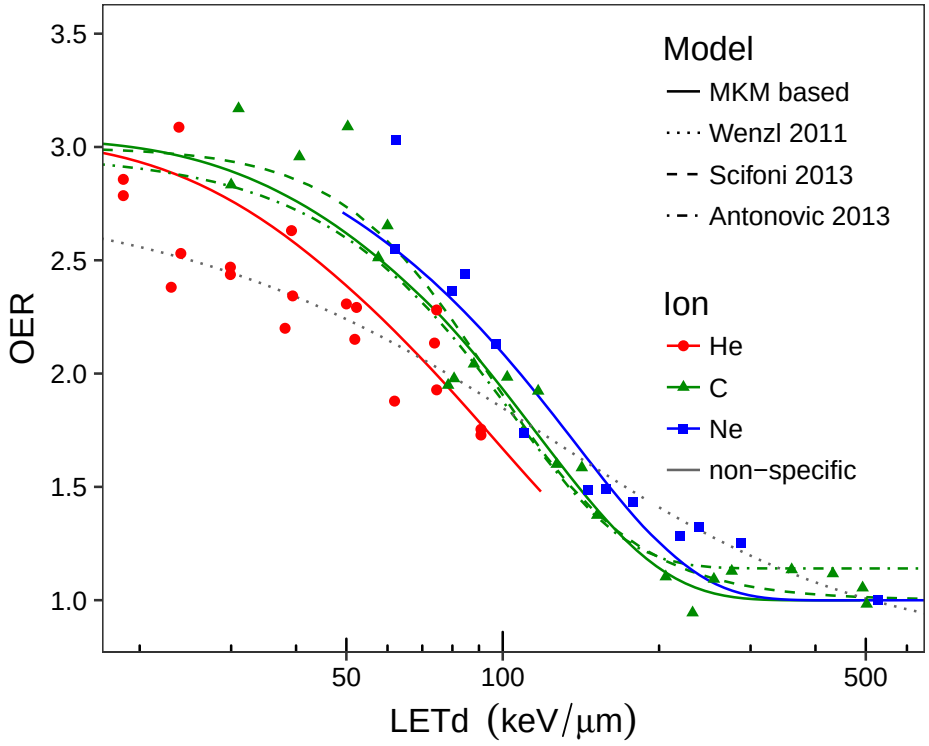

Figure 2. OER as a function of dose averaged LET for the irradiation of V79 cells with different ions. Points represent experimental data taken from (Furusawa et al. 2000). Continuous coloured lines represent the OER simultaneously evaluated by means of the MKM-based model for He, C and Ne. In the same plot the OER calculated with other models are reported for comparison (non-continuous lines). The models by (Scifoni et al. 2013) and (Antonovic et al. 2013) are associated with carbon ions only (green curve), while the model by (Wenzl & Wilkens 2011*a*) is not associated to a specific ion (grey curve.).

where ρ is the density of the medium and σ_N is the cross section of the nucleus, the OER predictions are sensibly worse. Specifically, by using the approximation 31 in place of equation 18, the differences among different ions are reduced and sensibly smaller than the differences observed in the experimental data. This is due to the fact that with this approximation only the ion dependence of the single-event averaged specific energy at the level of the domain (z_{1D}) is accounted for, while in our implementation the ion dependence is present in both z_{1D} and z_{1Dn}.

3.1.2. D_{10} analysis From the dataset reported in (Furusawa et al. 2000), it is possible to observe, for both HSG and V79 cells, a saturation of the D_{10} vs LET shifted to higher LET values in hypoxic conditions as compared to the aerobic conditions. The effect was also reproduced by the present model as shown in figure 3, where the hypoxic experimental data are reported along the model extrapolations to the hypoxic conditions.

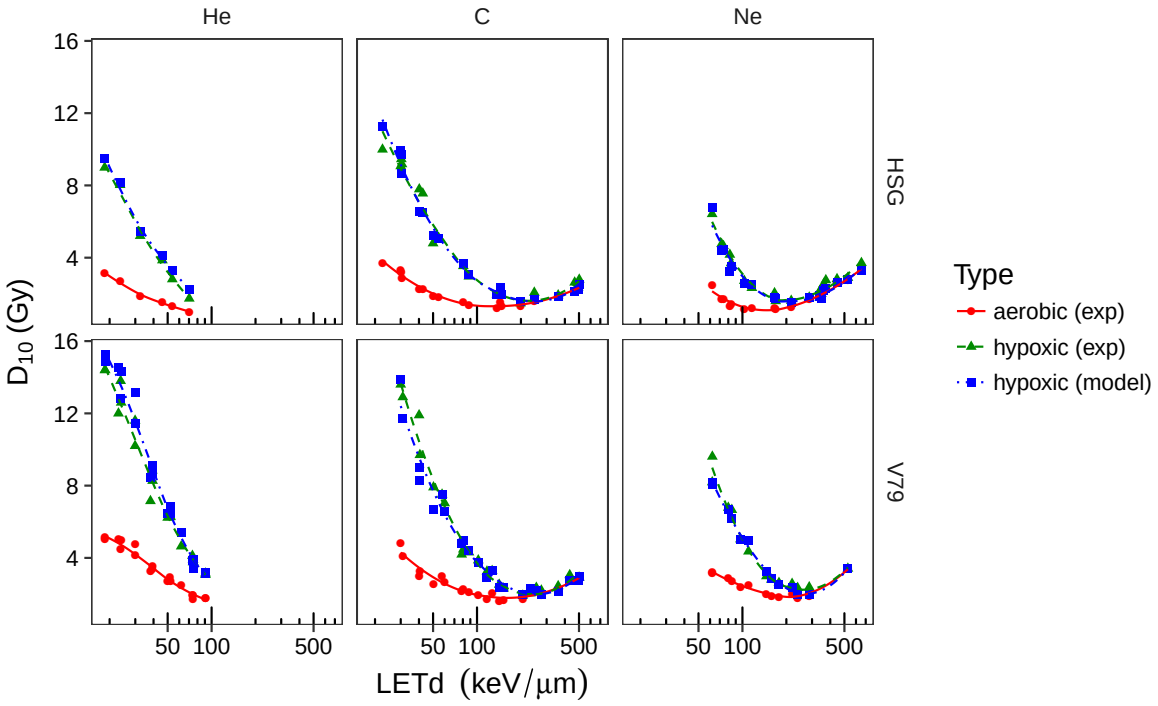

Figure 3. D_{10} as a function of dose averaged LET for the irradiation of HSG cells with different ions. Red points represent the aerobic experimental data while green points represent the hypoxic experimental data taken from (Furusawa et al. 2000). Blue points are the hypoxic D_{10} prediction performed by the model using the experimental aerobic data as a base reference. The continuous lines represent a smoothing of the discrete data performed via a loess algorithm.

3.1.3. Oxygen partial pressure dependence While the previous analysis has considered only fixed hypoxic and aerobic conditions, our model can be used to extrapolate the OER at different oxygen partial pressures. A comparison of the model with experimental data, taken from (Tinganelli et al. 2015), for CHO cells at different pressure conditions, is reported in figure 4. In these data the OER was measured at survival level 10% at 4 different oxygen concentrations for the hypoxic conditions (p_h = 0, 1.14, 3.8 and 15.2 mmHg) using different ions (C, O and N) at different dose-averaged LETs. The reference aerobic condition is p_a = 160 mmHg. The used model parameters for CHO cells are reported in table 1. In the same figure the predictions of the model described in (Tinganelli et al. 2015) are reported for comparison.

Figure 4 shows that the different values of p_h affect the OER. As expected, higher p_h values, corresponding to lower hypoxia level, give lower OER, while lower p_h values, related to high level of hypoxia, produce higher OER.

3.1.4. Dose dependence Usually, the values of the OER reported in literature correspond to a fixed survival level of 10%, neglecting the OER dependence on the applied dose. In order to see how our model modulates the OER as a function of the

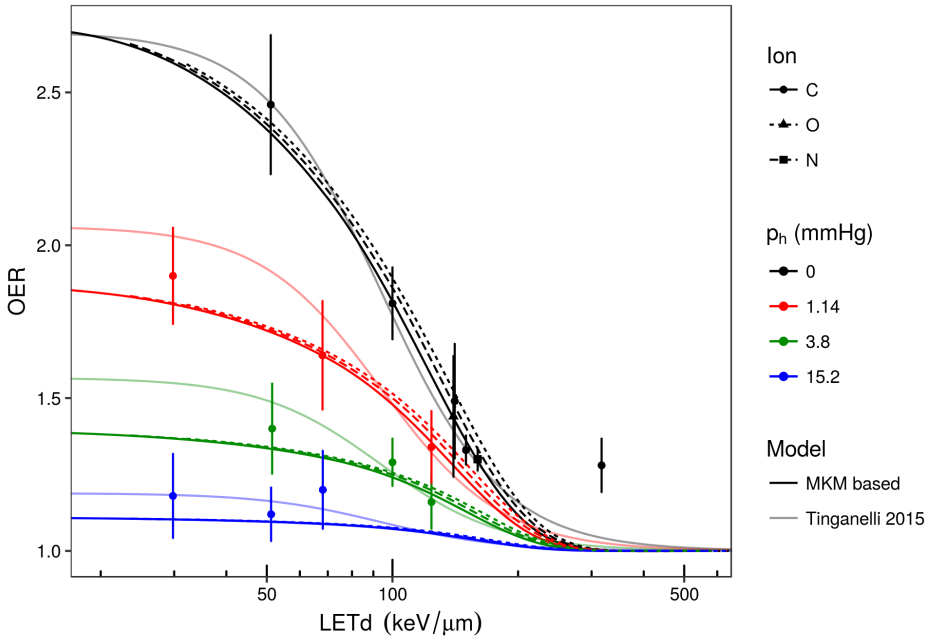

Figure 4. OER versus LETd for CHO cells, for different ion types and different values of oxygen partial pressure p_h. The partial pressure used for the reference aerobic condition is $p_a = 160$ mmHg. Dark lines correspond to the present MKM-based model while light lines correspond to the model reported in (Tinganelli et al. 2015).

applied dose, we performed comparisons between the OER vs dose curves evaluated by the model and those obtained from the experimental data (Furusawa et al. 2000) at different LETs. Both experimental and model evaluations were carried out through equation 3. In the former case the LQ parameters were independently fitted to the experimental survival curves for each available LET and for both aerobic and hypoxic conditions, while in the latter case they were directly evaluated by the model via equations 7, 8, 19−22. The hypoxic and aerobic reference oxygen partial pressures used for these evaluations are $p_h = 0.01$ mmHg and $p_a = 160$ mmHg respectively.

An example of this analysis is reported in figure 5, where the dose dependence of OER is reported for V79 cells irradiated with carbon ion at different LET, ranging from 30 to 502 keV/μm. The figure shows a general qualitative agreement between the model and the experimental curves. A general behaviour of OER vs dose can be evinced: the OER decreases with dose at low and intermediate LETs, with a maximum variation of $\sim 25\%$ for 30 keV/μm, whereas it stays almost constant for high LET. A similar behaviour has also been observed for HSG cells and other ions (He and Ne.) In particular, using the formalism introduced by Wenzl and Wilkens (see equation 7 in (Wenzl & Wilkens 2011*b*)), we obtain that the following relation holds for a significant majority of the LETs:

$$\mathrm{OER}(D \to 0) = \alpha_a/\alpha_h > \mathrm{OER}(D \to \infty) = \sqrt{\beta_a/\beta_h} \tag{32}$$

where the LQ parameters are directly fitted on the experimental survival curves. A

table and two additional plots, which detail these data, including the prediction of the LQ parameter ratios vs LET obtained using the present model, can be found in the supplementary materials (table 1S and figures 1S and 2S.) From these results it is possible to see that our model slightly underestimate the α and β ratios in the case of low LET carbon ions. This behaviour is consistent with the OER evaluations reported in figure 2 and 5.

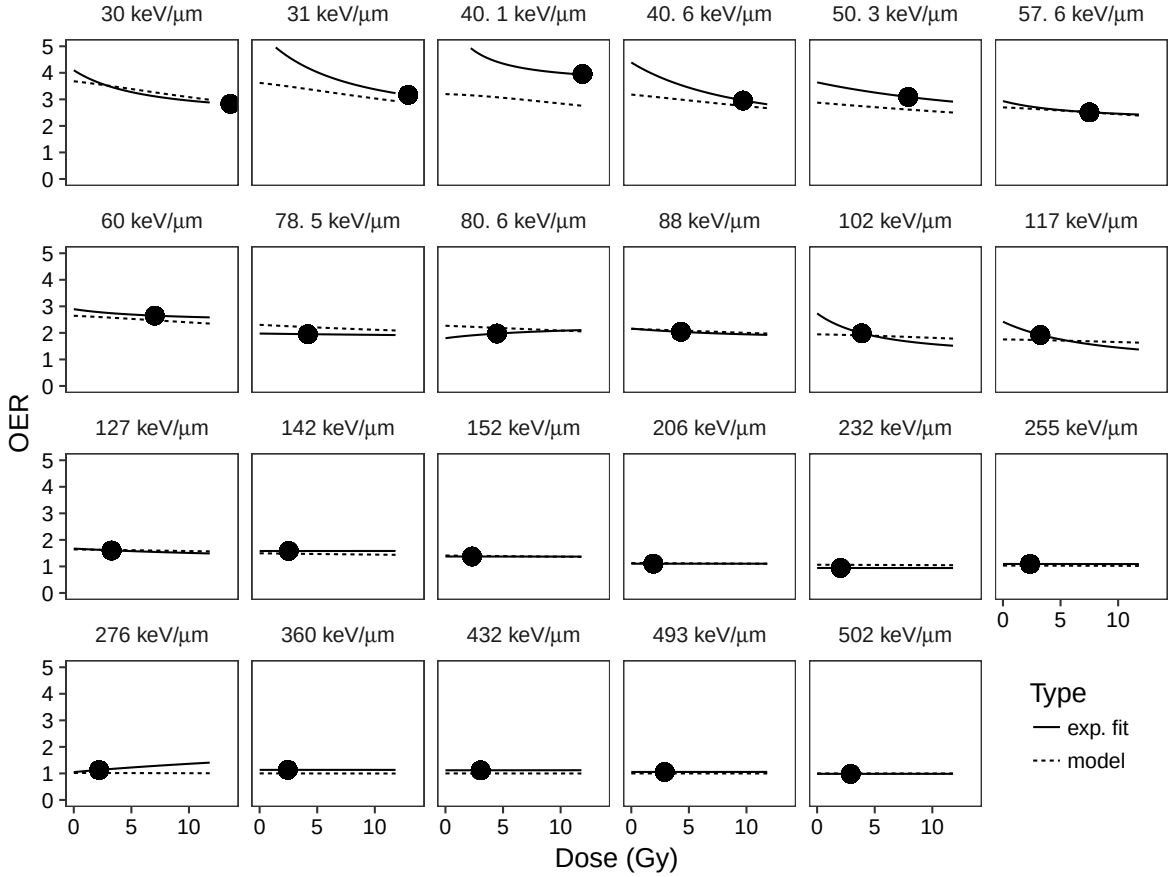

Figure 5. The extrapolated OER behaviour for V79 irradiated with C for different levels of dose. The dashed lines represent the extrapolation from the LQ parameters evaluated with the model, the straight lines represent the extrapolation form the LQ directly fitted to experimental data. The point represent the experimental value for a fixed survival level (10%) where the model was fitted (see also figure 2). Experimental data taken from (Furusawa et al. 2000).

3.2. Treatment simulations

3.2.1. SOBP in simplified geometries In figure 6 the OER profiles evaluated for different cubic SOBPs with sizes of 20, 40 and 60 mm (edges of the cubes), and for a unilateral irradiation with different ion types (H, He, Li, O) are reported. In the same figure the OER volume histograms evaluated in the target volume are also shown, for

different ions and target sizes. Based on these evaluations we found that the average OER in the target slightly increases when the target volume increases.

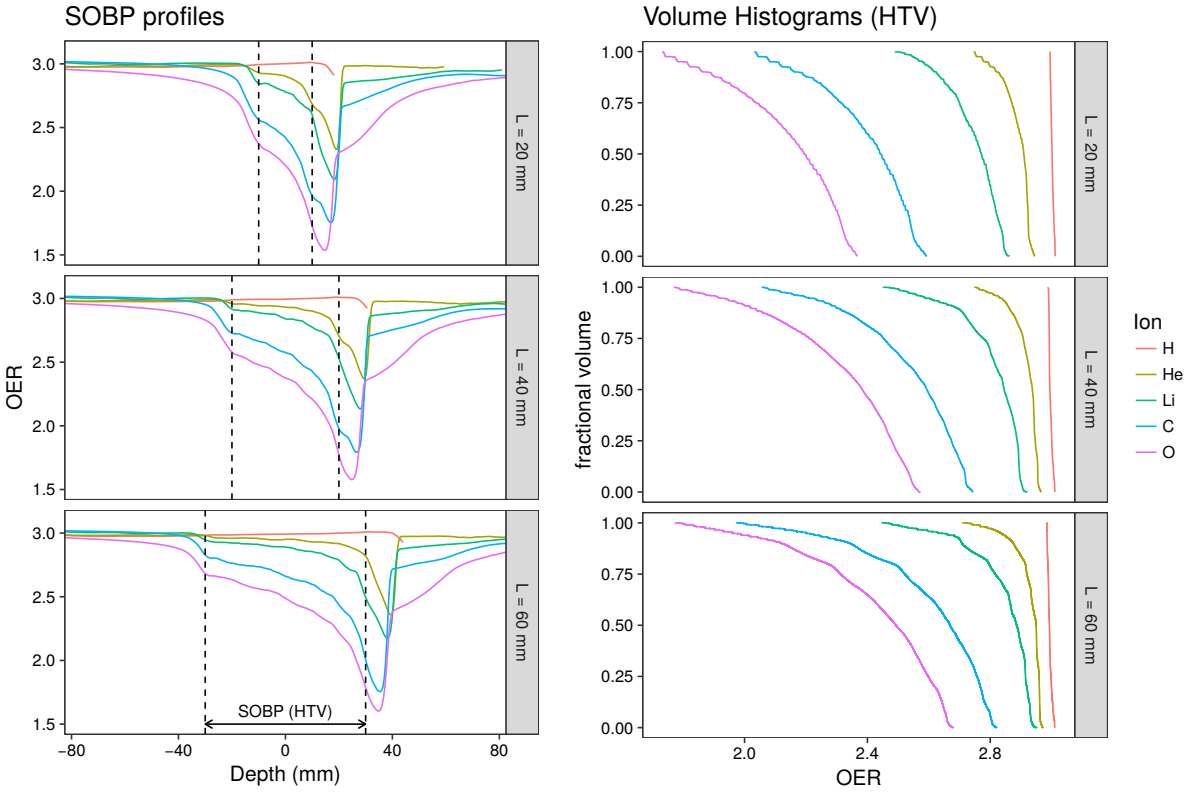

Figure 6. Left panels: OER profiles evaluated for the irradiation of H, He, Li, C and O ions for SOBP with different sizes. Right panels: volume histograms of the OER calculated in the target, for different ion types and for different SOBP sizes.

Considering the same unilateral irradiation with different ions, no significant average OER variations in the target volume among cubic SOBPs (20 mm) placed at different depth positions, corresponding to isocenters at −50, 0, and +50 mm, are observed (shown in figure 7.)

3.2.2. Clinical simulations Several clinical treatment simulations have been performed to evaluate the effects of the presence of a deficient oxygen region in the HTV. The beam setup and the dose distribution obtained in the case of proton irradiation with 2 Gy are reported in figure 8. In the same figure the localization of the PTV and the HTV is also shown.

A comprehensive overview of the HTV averaged OERs found for each treatment, evaluated with a varying oxygen partial pressure in the HTV, ranging from $p_h = 0.5$ mmHg to $p_h = 20$ mmHg, is reported in figure 9. The averaged OERs have been evaluated for the selection of ions (H, He, Li, C and O) and doses per fraction (2, 4, 6 and 8 Gy(RBE$_a$)) used in the treatment plans. This figure shows that the OER decreases for higher-LET ions, with an increase of the oxygen partial pressure in the

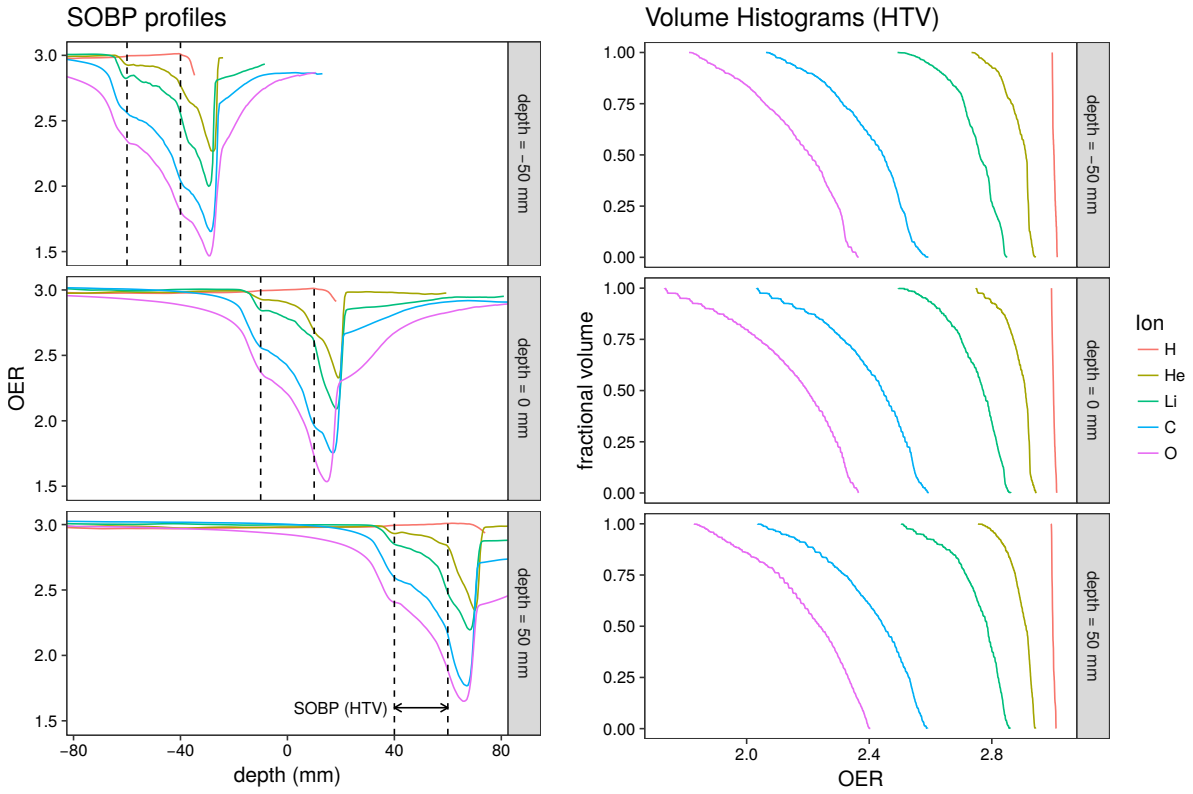

Figure 7. Left panels: OER profiles evaluated for the irradiation of H, He, Li, C and O ions for SOBP at different depths. Right panels: volume histograms of the OER calculated in the target, for different ions type and for different SOBP depths.

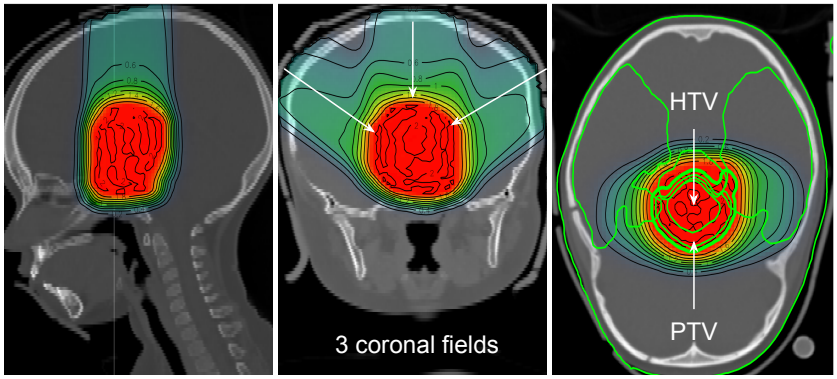

Figure 8. Irradiation setup for paediatric glioblastoma.

HTV and of the dose per fraction.

The TCP estimates are obtained for each combination of partial pressure, dose per fraction and primary ion. A comprehensive overview of the TCP as a function oxygen partial pressure in the HTV, for different doses per fraction, and for different primary ions is reported in figure 10. In this figure the reported TCP values correspond to a total dose of 72 Gy(RBE$_a$) with different doses per fraction and ion types.

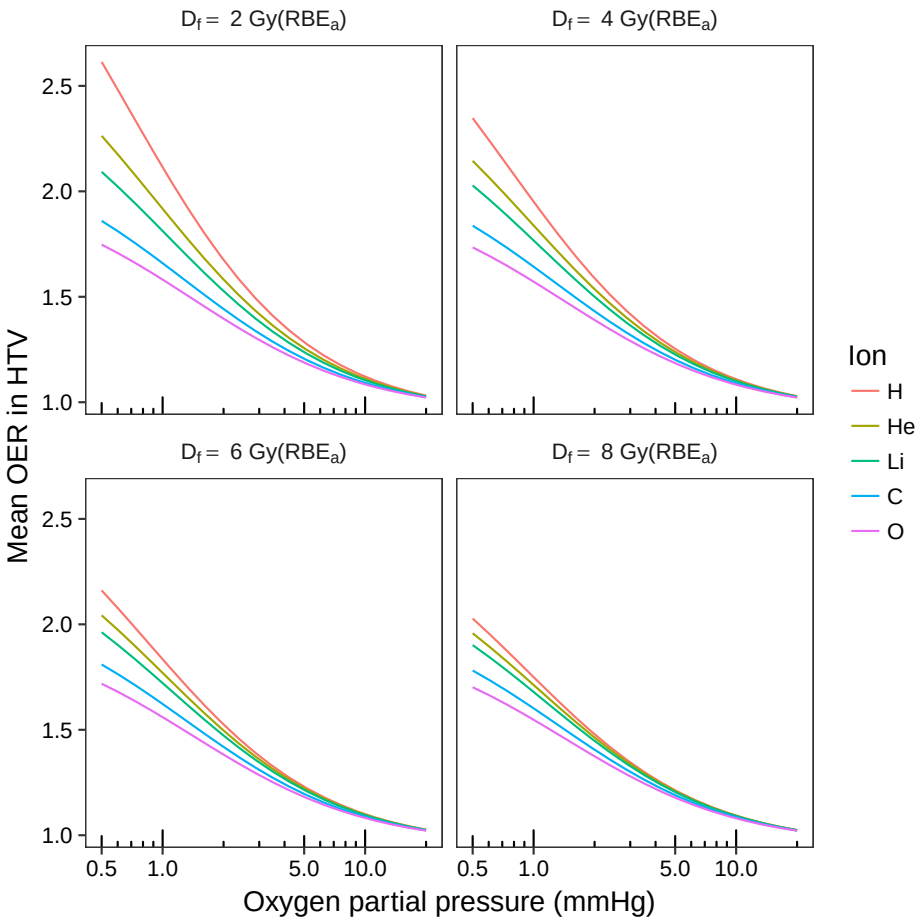

Figure 9. Volume averaged OERs versus oxygen partial pressure in the HTV, The OER is evaluated in the brain tumour PTV, for different ions type and RBE$_a$-weighted doses per fraction.

4. Discussion

4.1. Radiobiological effects modelling

4.1.1. LET and ion dependence The proposed model has been benchmarked against an experimental data set (Furusawa et al. 2000), consisting of 10% survival data for aerobic and hypoxic cells (V79 and HSG) irradiated with He, C and Ne. A good agreement have been found for the OER dependence on LET (figures 1 and 2), in particular for carbon ion data. Some discrepancies are observed in the case of He, where the model shows only a qualitative agreement with the dataset.

A comparison with other models (Wenzl & Wilkens 2011*b*, Scifoni et al. 2013, Antonovic et al. 2013) has also been carried out and reported in the same figures. A major deviation is observed in the case of (Wenzl & Wilkens 2011*b*). This deviation is likely due to the fact that the latter model has been optimized to reproduce with a single curve the OER reported in an ensemble of datasets, which include different

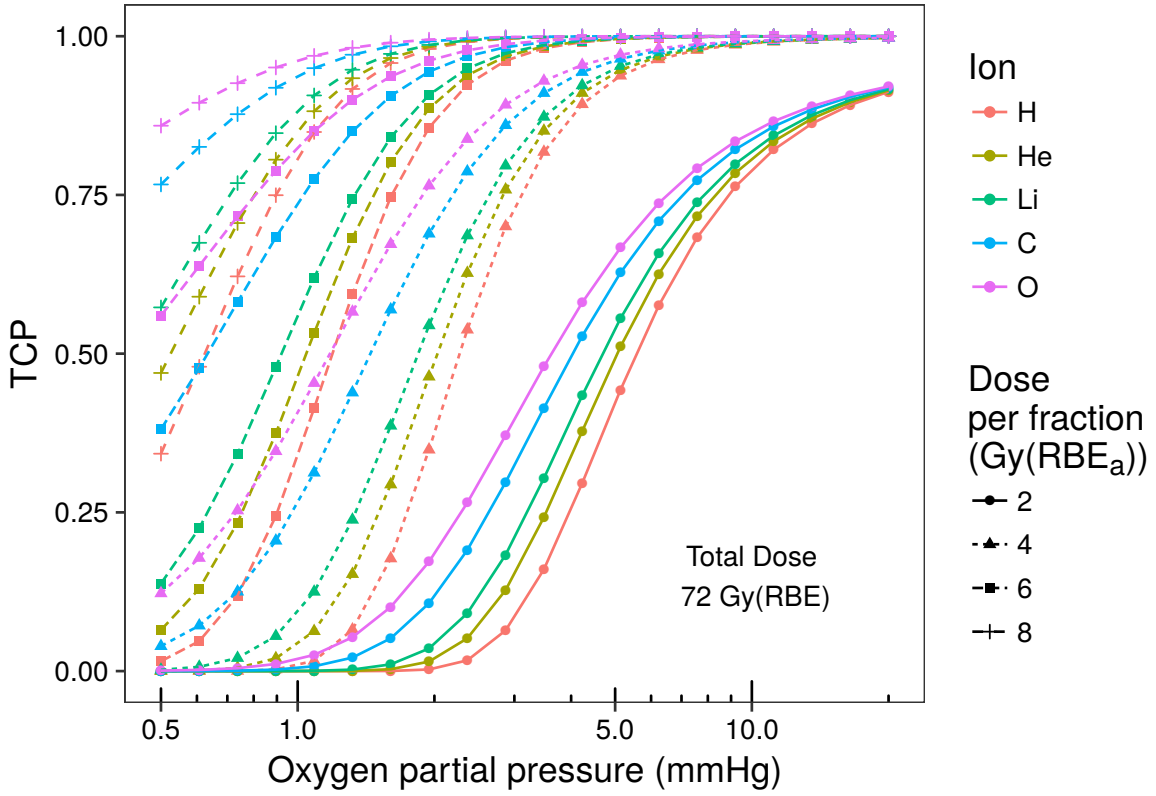

Figure 10. The TCP as a function of oxygen partial pressure in the HTV for different reference RBE$_a$-weighted doses per fraction (2, 4, 6 and 8 Gy (RBE$_a$)) and for different ion types (H, He, Li, C, O).

particles, ranging from x-rays to heavy ions. Conversely, the models presented in (Scifoni et al. 2013, Antonovic et al. 2013) have been optimized for carbon ions and their behaviour is similar to the one shown by the MKM-based model when limited to this ion. One of these models (Scifoni et al. 2013), has been in turn already compared with the one presented in (Stewart et al. 2011), showing a similar behavior.

The high OER values seen in the experimental data for LET $\to$ 0 (*e.g.* OER = 3.5 for HSG cells) are likely due to experimental fluctuations. Overall, similar saturation values of OER $\simeq$ 3 for both HSG and V79 in the limit LET $\to$ 0 were predicted by differents models (Wenzl & Wilkens 2011*a*, Stewart et al. 2011, Scifoni et al. 2013, Antonovic et al. 2013, Tinganelli et al. 2015, Bopp et al. 2016). A similar consistency has been observed also in the CHO data of (Tinganelli et al. 2015) reported in figure 4, where the experimental data and the models (our MKM-based model and the one described in the cited article) reasonably agree to a value OER $\simeq$ 2.7 for LET $\to$ 0, in the case of high hypoxia. Notably, in the case of the model implemented in (Scifoni et al. 2013, Tinganelli et al. 2015), the OER limit value is deliberately imposed, through a single explicit parameter, to the observed OER for photons (OER = 3 for V79 and HSG, OER = 2.7 for CHO). A similar strategy has been reported also in (Bopp et al. 2016)

where the OER saturation value has been adjusted to the observed photon OER for HSG (OER = 3.) Conversely, in the present model, there is no possibility to directly adjust the limit value of the model via an explicit parameter. This value depends on the interplay of other parameters and can be only extrapolated as a result of the fitting procedure along the complete LET range.

A major difference between the present model compared to the others (with the exception of (Bopp et al. 2016)) resides in the prediction of a different modulation of the OER as a function of LET according to the ion type. In particular, the present model predicts that the OER monotonically decreases as the LET increases and that the OER values for higher Z ions decrease in higher LET region compared to the low Z ions. This behaviour is consistent with the experimental observations. The ion dependence ultimately arises from the explicit inclusion of a specific track structure in the model. In this aspect, the present approach shares these features with the model proposed in (Bopp et al. 2016), in which a similar track modelling has been adopted (Kase et al. 2008). In particular, the usage of an explicit track structure allows the model to extrapolate the OER also to different ions, such as protons or Oxygen ions, not present in the experimental data set used in the fitting procedure. Although still qualitative due to lacking data, this predictive characteristics has been exploited in the present study, in the context of treatment simulations for ion beam therapy, where variable complex spectra and the contribution of secondary fragments were considered in the evaluation of the OER for the clinical treatments (see sections 2.2 and 4.2)

The choice of the track model and the MKM approximations introduced in the evaluation of the specific energies (see the observations reported in section 3.1.1) could affect significantly the predictions of the model, in particular those related to the OER ion dependence. Since the track model is mainly independent from the rest of the implementation, in principle it is possible to improve the agreement to the experimental data by using a different track model.

4.1.2. D_{10} analysis The D_{10} analysis shows that the model is also able to reproduce the behaviour of the D_{10} data from (Furusawa et al. 2000) with a good agreement. In particular the model reproduces the observed shift of the D_{10} minimum, found in the oxic condition, to higher LET, in case of hypoxia. These results are comparable with the ones reported in (Bopp et al. 2016).

4.1.3. Oxygen partial pressure dependence The Oxygen concentration analysis reported in figure 4 shows a good agreement between the behaviour of our model and the experimental data, comparable with the modelling approach used in (Scifoni et al. 2013, Tinganelli et al. 2015). In particular, as already discussed in section 4.1.1, the two modelling approaches show a similar value of OER in the limit LET $\rightarrow$ 0 (OER $\sim$ 2.7 for $p_h = 0$).

A small difference in the OER between ion types C, O and N in the LET range of 20 - 200 keV/μm is theoretically predicted by our model. The predicted difference

is small and it is also not appreciable in the scattered experimental data. We remark that the model predicts the OER dependence on the ion type to be more appreciable when comparing ions with relatively distant charges, such as carbon ions with respect to helium ions or protons. This behaviour is consistent with the experimental data shown in figures 1 and 2, where the difference among the ions (He, C and Ne) is more pronounced. As observed in (Tinganelli et al. 2015), the outlier point at high LET in figure 4 are probably due to the unfulfillment of the track-segment conditions or due to a contamination of nuclear fragments that is effectively reducing the actual LETd of the beam.

4.1.4. Dose dependence The analysis of the dependence of the OER on the applied local dose (see figure 5) shows an overall qualitative agreement between the model and the experimental curves, especially considering that the latter are extrapolations performed using the fitted LQ values with no available information about experimental uncertainties. Notably, the model is able to reproduce the vanishing dose dependence observed for intermediate to high LET range. This general behaviour is also consistent with the analysis shown in (Wenzl & Wilkens 2011*b*). However, in the same paper, an increasing OER for increasing dose is reported for the V79 cells (a decreasing OER vs dose is reported for T1 cells), while we observed a decreasing OER in both experimental data and model predictions, in particular for low to intermediate LETs. We remark that our findings have been confirmed by the analysis of the LQ parameter ratios (equation 32, see also table 1S and figures 1S and 2S.)

As already remarked in (Wenzl & Wilkens 2011*b*), there are many controversial findings for the dose dependence of OER, mainly due to the sensitivity of the fitted LQ parameters to the experimental noise and to the specific fitting procedure used in the analysis. We remark that, contrarily to the analysis performed in (Wenzl & Wilkens 2011*b*) in the case of V79 cells, where the mean values of the LQ parameters found in literature for two representative LET ranges (0.2-2 keV/um and 10-260 keV/um) were used, in the present study the experimental curves (continuous lines in figure 5) were obtained using directly the α and β values reported in (Furusawa et al. 2000), obtained by fitting directly and independently the survival curves of the hypoxic and aerobic cells for each available LET. These results show that a sensitivity analysis of the OER modelling could be a relevant issue to be addressed in further studies.

4.2. Treatment simulations

The proposed model can be potentially used to directly account for the aerobic and hypoxic cell survival data, *i.e.* to predict the oxygen partial pressure dependent LQ parameters, $\alpha = \alpha(p)$ and $\beta = \beta(p)$, without relying to a dose modifying factor, such as the OER (see equations 7, 8 and 19-22). This has the advantage to evaluate the accuracy of the model more strictly, with a direct comparison with respect the survival

data, being the OER a by-product of these computations. Another advantage is the possibility to have a survival- (or dose-) dependent OER.

Nevertheless, we chose to fit directly the OER data (combining the previous equations in 3), due to the strong noise in the LQ experimental data, in particular for the β parameter. The direct fit of the OER also permitted a more robust usage of the predicted OER to simulate the clinical conditions in the treatment planning study, where the absolute cell survivals of the irradiated tissues are substantially different from the cell survival observed in the *in vitro* experiment. This approach for the clinical OER is analogous to the RBE approaches used in therapy, in which the biological models provide only a relative modulation of the biological effect (c.f. equations 27 and 28).

An example of approach that try to directly account for survival data is described in (Bopp et al. 2016). A complementary approach, that couples the model directly to a dose modifying factor, such as the OER, is described in (Scifoni et al. 2013, Tinganelli et al. 2015). Other approaches that potentially can be linked to survival data, although these characteristics are not completely exploited, are given in (Wenzl & Wilkens 2011*a*, Brahme 2011, Antonovic et al. 2013).

4.2.1. SOBP in simplified geometries In this analysis the behaviour of OER has been investigated as a function of the type of particle and also considering hypoxic targets of various sizes placed a different depths.

The comparative analysis shows that the OER evaluated in the HTV is lower for high-LET ions and it is a decreasing function of depth along the direction of the irradiation in the HTV. Taking into consideration the differences in the investigated conditions, these results are in agreement with (Antonovic et al. 2014), reporting a decrease of the total dose to achieve the TCP of 50% from proximal to distal edge position of hypoxic target.

In the analysis of a cubic SOBP of variable volume we found that the average OER slightly increases when the target volume increases. This is an inherent size effect, due to the modulation of the LET in the SOBP. We remark that in this geometrical analysis we considered the SOBP to be coincident with the HTV. In particular, this effect is likely related to the fact that the high-LET distal region, in which the OER is lower, increases as $\sim L^2$, where L is the edge of the cube, while the low-LET proximal to middle region, in which the OER is higher, increases as $\sim L^3$. This inherent size effect represents a possible further modulation to the size effects expected when the hypoxia is considered only in a sub-region of the tumour and the size of this sub-region is changed, while the irradiated tumoural target volume is kept fixed. In the latter case a major impact on the tumour control is likely to be expected, as shown in (Bassler et al. 2014).

The comparative analysis of different SOBPs at different depths highlights that the depth at which the target volume is located does not significantly influence the OER.

4.2.2. Clinical simulations The comparative analysis of the clinical treatment simulations shows that the OER evaluated in the HTV is higher for low-LET ions (figure 9). The modulation of the OER among different ions is significant for lower oxygen concentrations for the hypoxic phase, while for $p_h > 2.5$ mmHg becames less significant. Our results support that higher-LET ions, such as carbon and oxygen ions, are convenient to treat hypoxic tumour as suggested in (Bassler et al. 2014).

A significant OER dependence on the dose per fraction has also been observed. Lower OER values have been found in case of hypofractionated regimes. This behaviour is more pronounced for low-LET than high-LET ions, consistently with the analysis presented in sections 3.1.4 and 4.1.4 where a less significant OER dose dependence is reported for higher LET. In particular, for high level of hypoxia ($p_h < 2.5$ mmHg), increasing the dose per fraction, from 2 to 8 Gy, the average OER found in the HTV is reduced by about 15%, in case of a treatment with protons. Such a scenario indicates that, in presence of hypoxia, a good plan of action to overcome the radioresistance induced by low oxygen concentration in tumour, could be offered by the use of hypofractionation.

As reported in figure 10, the TCP was found to be strongly dependent on the oxygen partial pressure in the HTV, the specific ion used in the treatment and the adopted fractionation scheme. In particular, consistently with the OER estimations reported in figure 9, higher tumour control is attained for high-LET ions and, in general, considering hypofractionation.

We remark that, as stated in section 2.2.3, in the present comparative study we optimized the plans using the RBE_a-weighted dose assuming aerobic conditions in the tumour. The idea behind this optimization choice is to provide a common starting point among the different plans in which normoxic conditions (for which OER = 1) are assumed. The hypoxia is then "switched on" and the behaviour among different treatments is analyzed systematically in terms of OER and TCP as functions of the oxygen partial pressure (figure 9 and figure 10). In particular this means that, for a given choice of RBE_a-weighted dose per fraction and RBE_a-weighted total dose, the TCP curves for different ions should converge in the same curve in the limit $p_h \to 30$ mmHg. The observed differences between the TCP curves for the different treatmens are likely heavily influenced by the non-linearity of this function. In particular they depends on the specific dose per fraction and total dose where the curves are evaluated.

From figure 11 is possible to visualize the features of the performed TCP analysis. In this figure the isolines of the TCP as a function of dose per fraction, D_f, and total dose, D_{tot}, both evaluated in $\mathrm{Gy}(\mathrm{RBE}_h)$, are reported. Notably, when D_f and D_{tot} are evaluated in $\mathrm{Gy}(\mathrm{RBE}_h)$, *i.e.* considering the hypoxia in the evaluation of the RWD (see equation 27), the function $\mathrm{TCP}(D_f, D_{\mathrm{tot}})$ corresponds to the photon TCP and it can be considered "universal" and ion-independent. From the figure it is possible to see how, by lowering the hypoxia oxygen partial pressure p_h, the different treatments (represented by points) move along the (D_f, D_{tot}) plane toward lower TCP values. In the case of $p_h = p_a = 30$ mmHg (normoxic conditions), the TCP depends only on

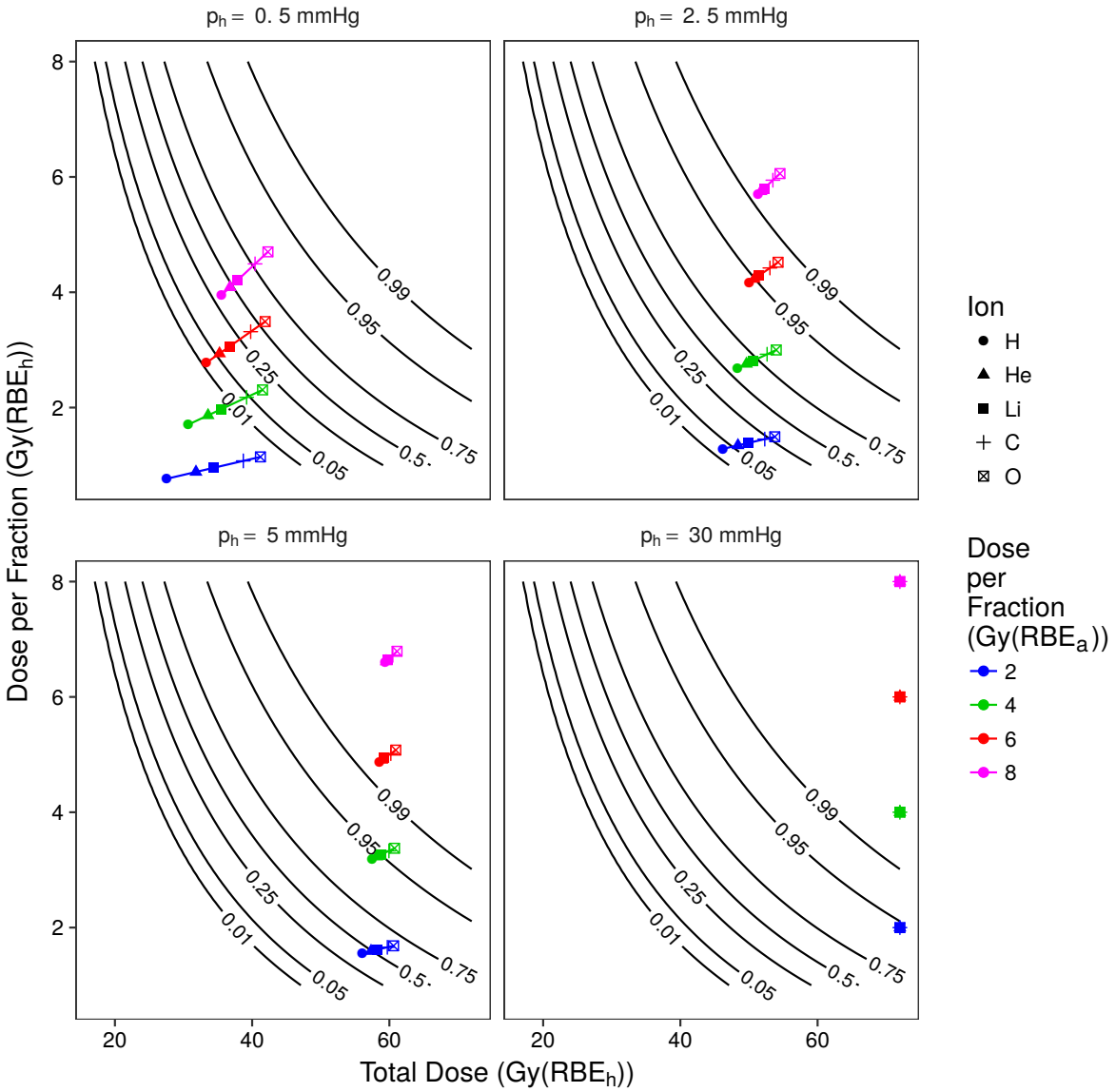

Figure 11. In this figure the isolines for the TCP as a function of the dose per fraction and the total dose (both in $\mathrm{Gy(RBE}_h)$) are reported as continuous black lines. The loci of the TCPs evaluated for different ions are represented by points with different shapes, and different doses per fraction in $\mathrm{Gy(RBE}_a)$ are represented by different colours. To guide the eye, the loci representing the same dose per fraction in $\mathrm{Gy(RBE}_a)$ are connected by a line. As in figure 10, the total dose is fixed to 72 $\mathrm{Gy(RBE}_a)$ for all the treatments. The four panels represent four different conditions of hypoxia, $p_h = 0.54$, 2.5, 5 and 30 mmHg.

the choice of dose per fraction and total dose, while, by decreasing the oxygen partial pressure p_h, the TCPs for different ions became distinct (the points separate from each other) and, for a given $p_h < p_a$, the deviations from the reference condition $p_h = p_a$ are more pronounced for light ions with respect the heavier ions. Furthermore, in this kind of visualization, the OER dose dependence is evinced when the points corresponding to

different doses per fraction and to the same ion are not vertically aligned. This happens in the case of light ions, while it is less visible in the case of carbon and oxygen ions, consistently with the analysis reported in figure 9.

4.2.3. Open issues Our works shows that the oxygen concentration and fractionation scheme could strongly affects the TCP rates. All these effects have been analyzed independently, in particular considering the oxygen concentration as static (non time-dependent) during the treatment. However, the fractionation schemes could modify the hypoxic status by permitting the reoxygenation due to the availability of oxygen after each fraction. This effect has not be fully considered in our study and could further improve the expected results as suggested in other papers. In particular, the effect of reoxygenation has been investigated for SBRT treatments suggesting a potential advantage for photon-based (Strigari et al. 2012) but also for carbon-ion treatments (Antonovic et al. 2014). The TCPs of hypoxic cells in the presence of local reoxygenation increase compared to those of hypoxic cells in static conditions (Antonovic et al. 2014). Moreover, the total dose to achieve the TCP of 50% growths with the number of fractions (Antonovic et al. 2014).

Among the strategies proposed to optimize the treatment plans accounting for hypoxia using high-LET ions (C and O), we cite the LET-painting approach (Bassler et al. 2010) based on the dose ramps combination procedure (Krämer & Jäkel 2005), the boost on hypoxic areas combined with LET painting (Bassler et al. 2014) and the OER-based optimizations (*kill painting*), in which the RBE_h-weighted dose (equations 27 and 28) is directly used to define biological constraints in the inverse planning procedure (Scifoni et al. 2013, Krämer et al. 2014, Tinganelli et al. 2015). Specific optimization strategies, accounting also for reoxygenation, will be investigated in further studies. In particular, in the current OER modelling, an oxygen partial pressure map defined at the voxel level can be used, accounting also for reoxygenation following the irradiations. A limit of the current OER evaluations is represented by the difficulty in providing a reasonable pressure map representing the actual specific hypoxic conditions of the patient during irradiation.

Finally, we remark that the results highlighted in the clinical analysis depend significantly to the specific parametrizations adopted for both the RBE and OER models and their interplay. As already pointed out in the previous sections, a general issue of OER modelling is the sensitivity of the model extrapolations on the experimental noise and the fitting procedure, in particular for high doses, due to the uncertainties associated to the β parameters. Moreover, the model has not been directly benchmarked against protons, Li or O due to the lack of available experimental data, apart few data points in (Tinganelli et al. 2015). Consequently, the results associated to the treatment planning simulations should be considered as a preliminary qualitative study, suggesting potential directions for further investigations.

5. Conclusions

This work proposes an approach for the OER evaluation based on the MKM, exploiting the general idea originally introduced by (Wenzl & Wilkens 2011*a*). The model takes into consideration the OER dependence from oxygen partial pressure, as suggested in (Alper & Howard-Flanders 1956) and the dependence of beta value from LET as assumed in the Local Effect Model (LEM) (Krämer & Scholz 2006). Moreover, following the work of (Kase et al. 2008) an amorphous track model obtained by the combination of the Kiefer model for the penumbra region (Kiefer & Straaten 1986) and the Chatterjee model for the core radius (Chatterjee & Schaefer 1976) has been implemented in the model. In addition, the beamlets superposition is carried out by applying the mixed-field formalism (Zaider & Rossi 1980) at the level of the single tracks.

The model has been compared with a set of experimental data (Furusawa et al. 2000, Tinganelli et al. 2015) and good agreements have been found. The model has been also used to evaluate the influence of hypoxia in a representative clinical case. Our results remark that hypoxia greatly influences treatment outcome and that the use of high-LET ion beams gives better tumour control. In particular it has been noted that in case of acute hypoxia conditions, combining the use of high-LET ions and/or an hypofractionated regime, an improvement of tumour control can be gained.

The model, which explicitly includes the dependence on ion type and dose per fraction, could be exploited to evaluate the impact of hypoxia in ion beam radiotherapy, facilitating the identification of the treatment condition optimality, including fractionation and primary particles selection. Next steps involve the usage of actual hypoxia distribution maps as a strategy to perform biological adaptive treatments.

Acknowledgements

This work has been partially supported by INFN CSN5 Call “MoVe IT”.

References

Alper T & Howard-Flanders P 1956 Role of Oxygen in Modifying the Radiosensitivity of E. Coli B. *Nature* **178**(4540), 978–979.

Ando K, Koike S, Ohira C, Chen Y J, Nojima K, Ando S, Ohbuchi T, Kobayashi N, Shimizu W & Urano M 1999 Accelerated reoxygenation of a murine fibrosarcoma after carbon-ion radiation. *International journal of radiation biology* **75**(4), 505–512.

Antonovic L, Brahme A, Furusawa Y & Toma-Dasu I 2013 Radiobiological description of the LET dependence of the cell survival of oxic and anoxic cells irradiated by carbon ions *Journal of Radiation Research* **54**(1), 18–26.

Antonovic L, Lindblom E, Dasu A, Bassler N, Furusawa Y & Toma-Dasu I 2014 Clinical oxygen enhancement ratio of tumors in carbon ion radiotherapy: The influence of local oxygenation changes *Journal of Radiation Research* **55**(5), 902–911.

Bassler N, Jäkel O, Søndergaard C S & Petersen J B 2010 Dose- and LET-painting with particle therapy. *Acta oncologica (Stockholm, Sweden)* **49**, 1170–1176.

Bassler N, Toftegaard J, Lühr A, Sø rensen B S, Scifoni E, Krämer M, Jäkel O, Mortensen L S, Overgaard J & Petersen J r B 2014 LET-painting increases tumour control probability in hypoxic tumours. *Acta oncologica (Stockholm, Sweden)* **53**, 25–32.

Bentzen S M & Tucker S L 1997 Quantifying the position and steepness of radiation dose-response curves. *International journal of radiation biology* **71**(5), 531–42.

Bopp C, Hirayama R, Inaniwa T, Kitagawa A, Matsufuji N & Noda K 2016 Adaptation of the microdosimetric kinetic model to hypoxia *Physics in Medicine and Biology* **61**(21), 7586–7599.

Brahme A 2011 Accurate Description of the Cell Survival and Biological Effect at Low and High Doses and LET's *Journal of Radiation Research* **52**(4), 389–407.

Chatterjee A & Schaefer H J 1976 Microdosimetric structure of heavy ion tracks in tissue. *Radiation and environmental biophysics* **13**(3), 215–227.

Furusawa Y, Fukutsu K, Aoki M, Itsukaichi H, Eguchi-Kasai K, Ohara H, Yatagai F, Kanai T & Ando K 2000 Inactivation of aerobic and hypoxic cells from three different cell lines by accelerated (3)He-, (12)C- and (20)Ne-ion beams. *Radiation Research* **154**(5), 485–496.

Hawkins R B 1998 A microdosimetric-kinetic theory of the dependence of the RBE for cell death on LET. *Medical physics* **25**(7 Pt 1), 1157–70.

Hawkins R B 2003 A microdosimetric-kinetic model for the effect of non-Poisson distribution of lethal lesions on the variation of RBE with LET. *Radiation research* **160**(1), 61–9.

Held K D 2006 Radiobiology for the Radiologist 6th ed., by Eric J. Hall and Amato J. Giaccia *Radiation Research* **166**(5), 816–817.

Hockel M, Knoop C, Schlenger K, Vorndran B, Baussmann E, Mitze M, Knapstein P G & Vaupel P 1993 Intratumoral pO2 predicts survival in advanced cancer of the uterine cervix *Radiotherapy & Oncology* **26**(1), 45–50.

Inaniwa T, Furukawa T, Kase Y, Matsufuji N, Toshito T, Matsumoto Y, Furusawa Y & Noda K 2010 Treatment planning for a scanned carbon beam with a modified microdosimetric kinetic model. *Physics in medicine and biology* **55**(22), 6721–37.

Jones B, Carabe-Fernandez A & Dale R G 2007 *in* R Dale & B Jones, eds, 'Radiobiological Modelling in Radiation Oncology' The British Institute of Radiology London pp. 138–57.

Kase Y, Kanai T, Matsufuji N, Furusawa Y, Elsässer T & Scholz M 2008 Biophysical calculation of cell survival probabilities using amorphous track structure models for heavy-ion irradiation. *Physics in medicine and biology* **53**(1), 37–59.

Kellerer A M & Rossi H H 1978 A Generalized Formulation of Dual Radiation Action *Radiation Research* **75**(3), 471–488.

Kiefer J & Straaten H 1986 A model of ion track structure based on classical collision dynamics. *Physics in medicine and biology* **31**(11), 1201–1209.

Krämer M & Jäkel O 2005 Biological dose optimization using ramp-like dose gradients in ion irradiation fields. *Physica medica* **21**(3), 107–11.

Krämer M & Scholz M 2006 Rapid calculation of biological effects in ion radiotherapy. *Physics in Medicine and Biology* **51**(8), 1959–70.

Krämer M, Scifoni E, Schmitz F, Sokol O & Durante M 2014 Overview of recent advances in treatment planning for ion beam radiotherapy *The European Physical Journal D* **68**(10), 306.

McKeown S R 2014 Defining normoxia, physoxia and hypoxia in tumours - Implications for treatment response *British Journal of Radiology* **87**(1035), 1–12.

Meesungnoen J & Jay-Gerin J P 2009 High-LET ion radiolysis of water: oxygen production in tracks. *Radiation research* **171**(3), 379–386.

Michael B D & Prise K M 1996 A multiple-radical model for radiation action on DNA and the dependence of OER on LET. *International journal of radiation biology* **69**(3), 351–358.

Munro T & Gilbert C 1961 The relation between tumour lethal doses and the radiosensitivity of tumour cells *Br J Radiol.* pp. 246–51.

Nakano T, Suzuki Y, Ohno T, Kato S, Suzuki M, Morita S, Sato S, Oka K & Tsujii H 2006 Carbon beam therapy overcomes the radiation resistance of uterine cervical cancer originating from

hypoxia *Clinical Cancer Research* **12**(7 I), 2185–2190.

Raju M R, Amols H I, Bain E, Carpenter S G, Cox R A & Robertson J B 1978 A heavy particle comparative study. Part III: OER and RBE *British Journal of Radiology* **51**, 712–719.

Russo G, Attili A, Battistoni G, Bertrand D, Cappucci F, Ciocca M, Mairani A, Molinelli S, Morone M C, Muraro S, Orts T, Patera V, Sala P, Schmitt E, Vivaldo G & Marchetto F 2016 A novel algorithm for the calculation of the physical and biological irradiation effect in scanned ion beam therapy : the beamlet superposition approach *Physics in Medicine & Biology* **183**, 1–31.

Scifoni E, Tinganelli W, Weyrather W K, Durante M, Maier A & Krämer M 2013 Including oxygen enhancement ratio in ion beam treatment planning: model implementation and experimental verification. *Physics in medicine and biology* **58**, 3871–95.

Stewart R D, Yu V K, Georgakilas A G, Koumenis C, Park J H & Carlson D J 2011 Effects of radiation quality and oxygen on clustered DNA lesions and cell death. *Radiation research* **176**(5), 587–602.

Strigari L, Benassi M, Sarnelli A & Polico R 2012 A modified hypoxia-based TCP model to investigate the clinical outcome of stereotactic hypofractionated regimes for early stage non-small-cell lung cancer (NSCLC) *Medical Physics* **39**(Lc), 4502–4514.

Thomlinson R H & Gray L H 1955 The Histological Structure of Some Human Lung Cancers and the Possible Implications for Radiotherapy *British journal of cancer* **9**(4), 539–549.

Tinganelli W, Durante M, Hirayama R, Krämer M, Maier A, Kraft-Weyrather W, Furusawa Y, Friedrich T & Scifoni E 2015 Kill-painting of hypoxic tumours in charged particle therapy *Scientific Reports* **5**, 17016.

Tinganelli W, Ma N Y, Von Neubeck C, Maier A, Schicker C, Kraft-Weyrather W & Durante M 2013 Influence of acute hypoxia and radiation quality on cell survival *Journal of Radiation Research* **54**(suppl 1), i23–i30.

Ward J F 1994 The complexity of DNA damage: relevance to biological consequences. *International journal of radiation biology* **66**(5), 427–432.

Wenzl T & Wilkens J J 2011*a* Modelling of the oxygen enhancement ratio for ion beam radiation therapy *Physics in medicine and biology* **56**(11), 3251–68.

Wenzl T & Wilkens J J 2011*b* Theoretical analysis of the dose dependence of the oxygen enhancement ratio and its relevance for clinical applications. *Radiation oncology (London, England)* **6**(1), 171.

Wouters B G & Brown J M 1997 Cells at intermediate oxygen levels can be more important than the hypoxic fraction in determining tumor response to fractionated radiotherapy. *Radiation research* **147**(5), 541–550.

Zaider M & Rossi H H 1980 The synergistic effects of different radiations. *Radiation research* **83**(3), 732–9.